Biomaterials 30 (2009) 3934–3945

Contents lists available at ScienceDirect

Biomaterials

journal homepage: www.elsevier.com/locate/biomaterials

The effect of Gd@$C_{82}(OH)_{22}$ nanoparticles on the release of Th1/Th2 cytokines and induction of TNF-α mediated cellular immunity

Ying Liu [a,1], Fang Jiao [b,1], Yang Qiu [a], Wei Li [b], Fang Lao [a], Guoqiang Zhou [b], Baoyun Sun [b], Genmei Xing [b], Jinquan Dong [b], Yuliang Zhao [a,b,*], Zhifang Chai [b], Chunying Chen [a,b,**]

[a] CAS Key Laboratory for Biomedical Effects of Nanomaterials and Nanosafety, National Center for Nanoscience and Technology of China, Beijing 100190, China
[b] CAS Key Laboratory for Biomedical Effects of Nanomaterials and Nanosafety and Key Laboratory for Nuclear Techniques, Institute of High Energy Physics, Chinese Academy of Sciences, Beijing 100049, China

ARTICLE INFO

Article history:
Received 21 March 2009
Accepted 1 April 2009
Available online 28 April 2009

Keywords:
Nanoparticle
Cytotoxicity
Immune response
Macrophage

ABSTRACT

It is known that down-regulation of the immune response may be associated with the progenesis, development and prognosis of cancer or infectious diseases. Up-regulating the immune response *in vivo* is therefore a desirable strategy for clinical treatment. Here we report that poly-hydroxylated metallofullerenol (Gd@$C_{82}(OH)_{22}$) has biomedical functions useful in anticancer therapy arising from immunomodulatory effects observed both *in vivo* and *in vitro*. We found that metallofullerenol can inhibit the growth of tumors, and shows specific immunomodulatory effects on T cells and macrophages. These effects include polarizing the cytokine balance towards Th1 (T-helper cell type 1) cytokines, decreasing the production of Th2 cytokines (IL-4, IL-5 and IL-6), and increasing the production of Th1 cytokines (IL-2, IFN-γ and TNF-α) in the serum samples. Immune-system regulation by this nanomaterial showed dose-dependent behavior: at a low concentration, Gd@$C_{82}(OH)_{22}$ nanoparticles slightly affected the activity of immune cells *in vitro*, while at a high concentration, they markedly enhanced immune responses and stimulated immune cells to release more cytokines, helping eliminate abnormal cells. Gd@$C_{82}(OH)_{22}$ nanoparticles stimulated T cells and macrophages to release significantly greater quantities of TNF-α, which plays a key role in cellular immune processes. Gd@$C_{82}(OH)_{22}$ nanoparticles are more effective in inhibiting tumor growth in mice than some clinical anticancer drugs but have negligible side effects. The underlying mechanism for high anticancer activity may be attributed to the fact that this water-soluble nanomaterial effectively triggers the host immune system to scavenge tumor cells.

1. Introduction

Cancer currently remains as one of the major causes of death worldwide, despite multiple approaches to therapy and prevention. Many kinds of tumors are characterized by a lack of early warning signs, diverse clinical manifestations and resistance to radiotherapy or chemotherapy. More importantly, many chemotherapeutic agents induce lymphopenia and down-regulate the immune system of patients. Chemotherapy and immunotherapy have always been used as independent forms of treatment, and conventional wisdom has been demonstrated that the two are antagonistic forms of therapy [1]. It is necessary to find an efficient nonsurgical agent to inhibit tumor growth, prevent tumor metastasis and delay tumor relapse.

The immune system is one of the most important means by which animals protect themselves from external threats, and plays a critical role in surveillance and prevention of malignancy. In recent years, immunotherapy has received more and more attention. The immune system is a collection of organs that protect against disease by identifying and killing pathogens and tumor cells. It is only when malignant cells develop mechanisms to escape the immune system that they become clinically significant tumors. Down-regulation of the immune response may result in further development of several kinds of tumors and infections. Up-regulating the immune response of tumor-bearing patients is a useful therapeutic approach. Nanoparticles are known to be able to interact with and affect the immune system [2]. The size, solubility and modified group of the nanoparticles affect the delivery of particles to immune cells and the outcome of tumor treatments. Nanoparticles in the range of 1–100 nm are frequently used

* Corresponding author.
** Corresponding author. Tel.: +86 10 82545560; fax: +86 10 62656765.
E-mail addresses: zhaoyuliang@ihep.ac.cn (Y. Zhao), chenchy@nanoctr.cn (C. Chen).
[1] These authors contributed equally to this work.

0142-9612/$ – see front matter © 2009 Elsevier Ltd. All rights reserved.
doi:10.1016/j.biomaterials.2009.04.001

experimentally for passive or active targeting of cancer cells. In particular, since their discovery in 1985, research on certain carbonaceous nanomaterials, such as fullerenes and their derivatives [3,4], has become an important field due to their unique chemical and physical properties. Though the solubility of fullerene in polar solutions is very poor, hydrophilic functional groups can be attached to the fullerene molecule to form water-soluble fullerene spherical molecules with hydrophilic functional groups, such as amido, carboxyl, poly-hydroxyl, or amide groups [4].

Research by Tabata and Ikada demonstrated a considerable effect of C_{60} bearing polyether side chains in shrinking skin cancer in mice based on the photo-induced generation of active oxygen, and indicated that PEG-modified C_{60} was a candidate agent for tumor therapy [5,6]. Gadolinium endohedral metallofullerenes were originally designed as a contrast agent in magnetic resonance imaging (MRI) for biomedical imaging [7]. However, recently it was demonstrated that $Gd@C_{82}(OH)_{22}$ nanoparticles could inhibit tumor growth more efficiently than prevailing chemotherapy drugs [8]. In addition, inhibition of virus growth by C_{60} derivative has also been reported [9]. However, present data do not fully understand the relationship between nanoparticles and the immune system. The remarkable biological property has attracted great attention.

Physicochemical properties such as nanoparticle size, surface charge, solubility, and surface functionality influence the function of immune system. For example, the immune responses can be enhanced by coat cationized galactose (cGal) on the surface of novel anionic engineered nanoparticles. cGal alone secreted very high levels of Th1 cytokines, but low levels of Th2 cytokines. In contrast, cGal-coated nanoparticles significantly enhanced both the Th1 and Th2 cytokines. It was believed that these engineered nanoparticles might have potential utility against pathogens that require both enhanced humoral and cellular-based immune responses [10]. When chitosan nanoparticles were coated with glucomannan, their delivery to immune cells increased. Perhaps the different surface functionality led to different phagocytic pathways to macrophages and dendritic cells, and different immune responses [11]. According to our previous experiments, $Gd@C_{82}(OH)_{22}$ nanoparticles had been shown to have anti-tumor effects, and morphological data obtained from HE-stained tumor tissues showed that the nanoparticles can improve immunity and interfere with tumor invasion in normal muscle tissue *in vivo* [8], suggesting that they may up-regulate the immune system.

Thus we design experiments to investigate the effect of $Gd@C_{82}(OH)_{22}$ nanoparticles on the immune system of tumor-bearing mice. The objectives are to investigate whether both the humoral and cellular immune responses are involved in reducing the growth and metastasis of tumors and which one is more important after administration of $Gd@C_{82}(OH)_{22}$ nanoparticles.

2. Materials and methods

2.1. Preparation and characterization of $Gd@C_{82}(OH)_{22}$ nanoparticles

2.1.1. $Gd@C_{82}(OH)_{22}$ nanoparticle preparation

Procedures for the preparation of water-soluble $Gd@C_{82}(OH)_{22}$ nanoparticles were as described previously [12]. In brief, $Gd@C_{82}(OH)_{22}$ nanoparticles were synthesized by the Krätschmer-Huffman method and extracted by a high temperature and high-pressure method. $Gd@C_{82}$ was separated and purified using high-performance liquid chromatography (HPLC, LC908-C60, Japan Analytical Industry Co), and identified by a matrix-assisted laser desorption time-of-flight mass spectrometer (MADLI-TOF-MS, Auto-Flex, Bruker Co., Germany). The mass spectrum was reported previously [8]. $Gd@C_{82}(OH)_{22}$ was synthesized by the alkaline reaction and purified by Sephadex G-25 column chromatography (5×50 cm^2) with an eluent of neutralized water.

2.1.2. $Gd@C_{82}(OH)_{22}$ nanoparticle characterization

Some characterizations of water-soluble $Gd@C_{82}(OH)_{22}$ nanoparticles were as described previously [8,12–16]. $Gd@C_{82}(OH)_{22}$ product was identified by a matrix-assisted laser desorption time-of-flight mass spectrometer (MADLI-TOF-MS), and the structure was determined using infrared spectroscopy and nuclear magnetic resonance (NMR). The hydroxyl number of each fullerene molecule was measured by synchrotron radiation X-ray photoelectron spectroscopy (XPS). The chemical form of the metallofullerenol used for the experiment *in vivo* was finally determined to be $Gd@C_{82}(OH)_{22}$ whose molecular mass was about 1516.

2.1.2.1. Zeta potential. $Gd@C_{82}(OH)_{22}$ molecules aggregated easily and formed nanoparticles in physiological solutions [13,14]. Zetasizer (Nano ZS90, Malvern, UK) was used to determine the surface charge of nanoparticles dispersed in phosphate buffered saline (PBS). The pH of the sample solutions was monitored using a standard laboratory pH meter, and all readings were conducted at room temperature.

2.1.2.2. Particle size measurements. The size of nanoparticles was measured using atomic force microscopy (AFM) (SPM-9500J3, Shimazu) and field emission scanning electron microscope (FE-SEM, Hitachi S-4800, Japan), while the size distribution of nanoparticles formed was characterized using dynamic light scattering (DLS) (Nano ZS90, Malvern, UK).

2.1.2.3. Stability in physiologically relevant media. For cell experiments *in vivo*, $Gd@C_{82}(OH)_{22}$ nanoparticles were diluted as needed with high-glucose Dulbecco's Modification of Eagles Media (DMEM) (Gibco, Grand Island, NY) containing 10% fetal calf serum (Gibco) and 2 mM L-glutamine, 20 mM HEPES, 100 U/mL penicillin, and 1 mg/mL streptomycin. To compare the stability in physiologically relevant media, the size distribution of $Gd@C_{82}(OH)_{22}$ nanoparticles dissolved in the medium and kept for 1 month at 4 °C, was measured using DLS.

2.2. Endotoxin determination of $Gd@C_{82}(OH)_{22}$ nanoparticles with LAL test

Endotoxin levels were determined using the *Limulus* amebocyte lysate test (LAL) [17]. The tachypleus amebocyte lysate (TAL) (number: 050113, sensitivity: $\lambda = 0.125$ EU/mL) was from Zhanjiang A&C Biological Ltd. (Zhanjiang, China). The control standard endotoxin (CSE) (government standard number: 200707, working standard number: 200862) and water (number: 050726) for the bacterial endotoxin test (BET) was provided by National Institute for the Control of Pharmaceutical and Biological Products (Beijing, China).

After repeated examination of TAL sensitivity and sample interference test, four tubes with 0.1 mL TAL reagent were used 0.1 mL $Gd@C_{82}(OH)_{22}$ aqueous solution (100 μM) was added to two tubes, meanwhile 0.1 mL BET water and 0.1 mL working CSE were added to the other two tubes as negative control and positive control. All tubes were incubated for 1 h in a water bath at 37 ± 1 °C. After the test tube was inverted 180° slowly, it is positive and recorded as (+) if the gel in tube is not deformed and does not slip from the wall, whereas is negative and recorded as (−). Test is invalid when positive control is (−) or negative control is (+).

2.3. Isolation and preparation of primary immune cells including B and T lymphocytes and macrophages

Inbred female C57BL/6 mice were used as recipients in this study. The mice were approximately 6 weeks' old with body weights in the range of 18.0–20.0 g, and were provided by the Laboratory of Experimental Animals of the Chinese Academy of Medical Sciences.

Total spleen cells were prepared from healthy mice according to a standard published method [18]. Fresh spleens were aseptically removed, placed in cold PBS, and immediately homogenized. The homogenate was filtered through a stainless steel gauze to remove tissue debris. Cells were then applied to Ficoll–Hypaque and centrifuged at 600 g for 30 min to remove red blood cells. Lymphocytes were collected and washed twice (250 g, 10 min) with PBS.

B and T lymphocytes were isolated using magnetic cell sorting (MACS) microbeads (BD Bioscience Pharmigen, San Diego, CA) and suspended in the complete medium (DMEM containing 10% fetal calf serum and 2 mM L-glutamine, 20 mM HEPES, 100 U/mL penicillin, and 1 mg/mL streptomycin), at 37 °C in humidified incubators (Thermo Forma, USA) with 5% CO_2.

Macrophages, present in high numbers among peritoneal cells, were harvested according to a previously published method [18,19]. Briefly, PBS containing 10% inactivated fetal calf serum (pH 7.2) was injected intraperitoneally. After 30 s, peritoneal macrophages were collected with a Pasteur pipette, and resuspended in complete medium. Cells were seeded onto plastic tissue culture flasks for 1 h to allow macrophages to adhere, and nonadherent cells were removed by extensive washing.

2.4. Flow cytometric analysis of T cell surface markers

Monoclonal antibodies against CD_4 and CD_8 conjugated with different fluorochromes (BD Bioscience Pharmigen, San Diego, CA) were used for staining splenocyte surface markers. 1×10^5 total spleen cells were incubated for 30 min at room temperature with phycoerythrin (PE)-conjugated anti-mouse CD_4 monoclonal antibody and a fluorescein isothiocyanate (FITC)-conjugated anti-mouse CD_8 monoclonal antibody, both of which were diluted 1:100 (volume/volume) in PBS with 2% BSA. After 3 washes, samples were resuspended in PBS and analyzed with a BD FACSCalibur flow cytometer. Results are given as the percentage of positively

stained cells. The ratios of CD_4^+/CD_8^+ T cells from different groups are shown on representative histograms.

2.5. Incubation of tumor cells (LLC cells) and primary immune cells with $Gd@C_{82}(OH)_{22}$ nanoparticles

Lewis lung carcinoma (LLC) cells were purchased from the Laboratory of Experimental Animals of the Chinese Academy of Medical Sciences and cultured in complete medium. LLC cells and primary immune cells, including B and T lymphocytes and macrophages, were cultured in the presence of $Gd@C_{82}(OH)_{22}$ nanoparticles in 96-well plates at 37 °C, in a humidified atmosphere of 5% CO_2 for 1 h, 6 h, 12 h, 24 h, 48 h and 72 h. The concentration of $Gd@C_{82}(OH)_{22}$ nanoparticles in incubation solutions was 0.1 μM, 1 μM, 10 μM and 100 μM. Normal cultured cells were used as negative controls. The density of LLC cells, B and T lymphocytes and macrophages was 1×10^4 cells/well, 4×10^5 cells/well, 4×10^5 cells/well and 2×10^5 cells/well. After incubation, the cells were washed, collected by centrifugation, and resuspended in cell culture medium.

2.6. Cell viability and cytotoxicity assays

Cell viability was determined by trypan blue exclusion. LLC cells, B and T lymphocytes and macrophages were separated by centrifugation from the complete medium before assaying. Cell numbers and viability were assessed both at the beginning and at the end of the assays.

A cell count kit-8 (CCK-8) (Kumamoto Techno Research Park, Japan) was used to examine cell proliferation. CCK-8 includes WST-8 [2-(2-methoxyl-4-nitrophenyl)-3-(4-nitrophenyl)-5-(2,4-disulfonicacid benzene)-2*H*-tetrazalium sodium] which can be reduced to highly water-soluble formazan dye which is yellow. Briefly, cells were incubated in the presence of $Gd@C_{82}(OH)_{22}$ nanoparticles with 100 μL of culture medium in 96-multiwell plates. Media were removed and 100 μL DMEM containing CCK-8 (10%) was added to each well. After a 2 h incubation at 37 °C, the absorbance at 450 nm of each well was measured using a standard enzyme-linked immunosorbent assay (ELISA)-format spectrophotometer. Each experiment was repeated three times, and data represented the mean of all measurements.

2.7. Detection of apoptosis and necrosis

Apoptotic cells and necrotic cells were analyzed by double staining with annexin V-FITC and propidium iodide (PI), in which annexin V bound to apoptotic cells with exposed phosphatidylserines (PS), while PI labeled necrotic cells with membrane damage. One of the earliest indications of apoptosis is the translocation of the membrane phospholipid PS from the inner to the outer leaflet of the plasma membrane. Once exposed to the extracellular environment, binding sites on PS become available for annexin V, a 35 kDa Ca^{2+}-dependent, phospholipid-binding protein with a high affinity for PS. Healthy cells were double negative, early apoptotic cells were positive for annexin V staining but negative for PI staining, while late apoptotic cells were double positive. Cells stained with PI only were considered to be necrotic rather than apoptotic.

In this study, LLC cells and primary immune cells were incubated with $Gd@C_{82}(OH)_{22}$ nanoparticles at a concentration of 100 μM for 72 h. After incubation, adherent cells were harvested by trypsinization and all cells (floating and adherent) were washed once with cold PBS and pelleted at 1000 rpm. Annexin V-FITC was added to the cell suspension in the presence of binding buffer and incubated for 20 min at room temperature. Cells were co-stained with PI and immediately analyzed by a Beckman Coulter Cell Lab Quanta™ SC (America). The percentage of apoptotic (annexin+/PI−) and necrotic (annexin+/PI+) cells was determined using Quanta™ SC software. Data represent the mean fluorescence obtained from a population of 10,000 cells.

2.8. Detection of cytokines in culture supernatants

A BD Mouse Th1/Th2 Cytokine CBA Kit was used to quantitate IL-2, IL-4, IL-5, IFN-γ and TNF-α protein levels in cell culture supernatants. B and T lymphocytes and macrophages were divided into 4 groups: (1) normal cultured cells were used as negative controls, (2) lipopolysaccharide (LPS, 100 ng/mL) stimulated cells were used as positive controls, (3) cells treated with $Gd@C_{82}(OH)_{22}$ nanoparticles at a concentration of 100 μM and cultured for 72 h, (4) cells incubated with LPS at 100 ng/mL for 24 h after pre-culture with 100 μM $Gd@C_{82}(OH)_{22}$ for 48 h. Physiologically relevant concentrations (pg/mL) of specific cytokine proteins were estimated. The density of B and T lymphocytes and macrophages was 4×10^5 cells/well, 4×10^5 cells/well and 2×10^5 cells/well, respectively.

2.9. ELISA determination of IL-6 levels in culture supernatants

Levels of IL-6 in culture supernatants for B and T lymphocytes and macrophages were determined by a specific ELISA according to the manufacturer's instructions, using matched antibody pairs and recombinant cytokines as standards (BD Bioscience Pharmigen, San Diego, CA). Briefly, 96-multiwell plates coated with the corresponding purified anti-mouse capture monoclonal antibody were used. Culture supernatants and serial dilutions of the standard were added to each well and incubated for 90 min at 37 °C. After four washes, bound samples were detected using the corresponding biotinylated anti-mouse antibody at 37 °C for 1 h. After another four washes, avidin-horseradish peroxidase solution was added, and plates were incubated at 37 °C for 30 min. After the final four washes, plates were kept at 37 °C for 20 min to react with the substrate solution. 100 μL of blocking solution was added to stop the reaction, and the absorbance at 450 nm was then recorded. Results were expressed in pg/mL, and three independent experiments were performed.

2.10. Animals

Inbred female C57BL/6 mice with body weights in the range of 18.0–20.0 g were used as recipients in this study, and housed in a temperature-controlled, ventilated and standardized disinfected animal room. Mice were allowed to acclimatize, without handling, for a minimum of 1 week before the start of experiments. All animal experiments were conducted using protocols approved by the Institutional Animal Care and Use Committee at the Institute of Tumors of the Chinese Academy of Medical Sciences.

2.11. In vivo anti-tumor experiment

Forty mice were divided randomly into 4 groups, with one group of normal controls not receiving any treatment, while the remaining 30 mice were used for the tumor-bearing study. Tumor-bearing mice, which had been injected subcutaneously with 1×10^6 LLC cells in the right upper hind leg, were administered intraperitoneally with either 0.2 mL saline, 0.1 or 0.5 μmol/kg $Gd@C_{82}(OH)_{22}$ nanoparticles, once a day before sacrifice.

Tumor diameter was measured using calipers once a day. The experiment was discontinued when the tumor diameter reached 2 cm. After sacrificed, mice were weighed before and after tumor tissue was removed, blood samples taken from the retroorbital sinus of the mice were centrifuged at 4000 rpm for 15 min at 4 °C to obtain serum, meanwhile, tumor and organ samples (heart, liver, spleen, kidney and lung) were surgically removed rapidly and weighed. Tumor volumes were calculated according to the following equation [20]: tumor volume (mm^3) = $1/2 \times a \times b \times b$ (where '*a*' is the vertical long diameter and *b* is the vertical short diameter). Tumor inhibition rates were calculated using the following formula: rate of inhibition (%) = (mean tumor weight of untreated saline control − mean tumor weight of treated group)/mean tumor weight of untreated saline control × 100. And the organ weight coefficient (%) = organ weight (mg)/mouse body weight (g) × 100.

2.12. Histopathological analysis of tumors

Immediately after surgical removal, tumors were fixed overnight in 10% formalin neutral buffer, dehydrated in a series of graded ethanol solutions and embedded in paraffin. Baseline histological slides containing sections (4-5 μm in thickness) were stained with hematoxylin/eosin (HE) and examined blindly by a well-trained pathologist. Histological observations and photomicrography were performed using a light microscope (Nikon U-III multipoint sensor system).

2.13. Content of Gd element in tumor samples

Tumor samples were weighed, digested and analyzed for Gd content according to a conventional procedure [21]. Inductively coupled plasma-mass spectrometry (ICP-MS, Thermo Elemental X7, Thermo Electron Co.) was used to analyze the Gd concentration in each sample. Indium of 20 ng/mL was regarded as an internal standard element. The detection limit of Gd was 1.47 pg/mL. Briefly, tumors were soaked in nitric acid overnight and heated at about 80 °C. H_2O_2 solution was used to drive off the vapor of nitrogen oxides until the solution was colorless and clear. After the solution volume was fixed to 3 mL using 2% diluted nitric acid, Gd content was analyzed using ICP-MS.

2.14. Detection of cytokines in mouse serum and tumor samples

The following procedures were performed to prepare tumor homogenates [21]. After washing three times with 0.01 M Tris–HCl buffer (0.01 M Tris–HCl, 0.0001 M EDTA-Na_2, 0.01 M sucrose, 0.8% NaCl, pH 7.4), the tumor tissues were homogenized at 4 °C with an Ultrasonic Processor (Sonics, Vibra cell, USA). The supernatants collected were used for measurement of cytokine levels as following.

Cytokines in mouse sera and 10% tumor homogenates including Interleukin-2 (IL-2), Interleukin-4 (IL-4), Interleukin-5 (IL-5), TNF-α and Interferon-γ (IFN-γ) were measured quantitatively using a BD™ cytometric bead array mouse Th1/Th2 cytokine CBA kit (BD Bioscience Pharmigen, San Diego, CA) following the manufacturer's instructions. Five bead populations with distinct fluorescence intensities were coated with capture antibodies specific for IL-2, IL-4, IL-5, IFN-γ, and TNF-α proteins. The cytokine beads mixed together were added to the appropriate assay tubes. Mouse Th1/Th2 cytokine standard dilutions were added to control tubes while mice serum and 10% tumor homogenates were added to the remaining tubes. After mouse Th1/Th2 PE detection reagent was added, assay tubes were protected from direct exposure to light and incubated for 2 h at RT. After washing, the beads were

resuspended using wash buffer. All beads were then analyzed using a BD FACSCalibur flow cytometer and BD Cell Quest software. Data were formatted and analyzed further using BD CBA software. Physiologically relevant concentrations (pg/mL) of specific cytokine proteins were estimated.

2.15. Statistical analysis

Results were expressed as means ± standard deviations (SD). The statistical significance of the observed differences was analyzed by *t*-tests or one-way analysis of variance (ANOVA) followed by the Student–Newman–Keuls test. A p value < 0.05 was considered to be significantly different.

3. Results

3.1. Structure and characterization of Gd@$C_{82}(OH)_{22}$

Gd@$C_{82}(OH)_{22}$ nanoparticles were synthesized and characterized as described previously [8,12–16]. The average number of hydroxyls was 22 as determined by XPS, and a schematic drawing of a Gd@$C_{82}(OH)_{22}$ molecule was shown in Fig. 1A. According to results of the previous experiments, the size of the Gd@$C_{82}(OH)_{22}$ molecule itself was less than 2 nm [8], but Gd@$C_{82}(OH)_{22}$ tended to aggregate in aqueous solutions (pH 7.0) and formed dispersed Gd@$C_{82}(OH)_{22}$ nanoparticles with an average diameter of 100 nm as determined by SEM (Fig. 1C) and AFM (Fig. 1D). The average diameter of Gd@$C_{82}(OH)_{22}$ nanoparticles determined by DLS was 91.8 ± 9.5 nm, in agreement with those obtained by SEM and AFM.

The zeta potential is a measure from the electrical charge of the surface and a predictive value for the interfacial reactions between the biomaterial and the surrounding tissue [22,23]. Fig. 1B showed the effect of lowering the pH from 7.0 to 3.0 and of increasing the pH from 7.0 to 10.0 on the zeta potentials of Gd@$C_{82}(OH)_{22}$ nanoparticles prepared in 0.01 M PBS. Both the lowering and increasing pH would induce an increase of zeta potentials of Gd@$C_{82}(OH)_{22}$ nanoparticles. These results indicated that the Gd@$C_{82}(OH)_{22}$ nanoparticles were stable in PBS of pH 7.0, 8.0, 9.0 and became unstable under lower and higher pH conditions. In both the *in vivo* and *in vitro* experiments, pH of Gd@$C_{82}(OH)_{22}$ nanoparticles solution was 7.0–.0, which is a pH range of very stable nanoparticles.

To observe the nanoparticle stability in physiological media, the size distribution of Gd@$C_{82}(OH)_{22}$ nanoparticles kept in the complete medium for 1 month at 4 °C was measured using DLS. The average diameters of Gd@$C_{82}(OH)_{22}$ nanoparticles before and after being kept were 154.0 ± 68.5 nm (Fig. 1E) and 157.5 ± 76.4 nm (Fig. 1F), respectively. That is to say, Gd@$C_{82}(OH)_{22}$ nanoparticles were stable in the physiological media.

3.2. Effect on CD_4^+ to CD_8^+ T cells

Total spleen cells isolated from healthy mice were cultured in 6-well plates in the presence of Gd@$C_{82}(OH)_{22}$ nanoparticles at a concentration of 100 μM for 1 h, 6 h, 12 h, 24 h, 48 h and 72 h. Normal cultured cells were used as negative controls. After incubation for 1 h, 6 h, 12 h and 24 h, the ratio of CD_4^+ to CD_8^+ T cells was unchanged ($p > 0.05$). However, the ratio of CD_4^+ to CD_8^+ T cells increased significantly after 48 h ($p < 0.05$) (Fig. 2). Thus, CD_4^+ T cells may play an indispensable role in anti-tumor immunology.

3.3. Effects on the immune cells

CD_4^+ T cells can be divided into two subsets: Th1 and Th2. Th1 cells mainly secrete IL-2, IL-12, IFN-γ, TNF-β and other Th1-type cytokines, inducing cell-mediated immunity to activate cytotoxic T-cells and macrophages. Th2 cells mainly secrete IL-4, IL-5, IL-6, IL-10, IL-13 and other Th2-type cytokines, inducing humoral immunity to activate B cells and eosinophils and produce IgE. The balance between Th1 and Th2 cells, related to a variety of diseases, is associated with infectious diseases, allergic diseases, autoimmune diseases, and the progenesis, development and prognosis of cancers. We hence investigated the influence of Gd@$C_{82}(OH)_{22}$ nanoparticles on CD_4^+ T cells.

3.3.1. Activation of the immune cells

To further confirm the effect of Gd@$C_{82}(OH)_{22}$ nanoparticles on the immune system of tumor-bearing mice, primary immune cells, including B and T lymphocytes and macrophages, were isolated and cultured together with 100 μM Gd@$C_{82}(OH)_{22}$ nanoparticles for 48 h. Secretion of cytokines IL-2, IL-4, IL-5, IL-6, TNF-α and IFN-γ in the culture supernatant was assayed with ELISA and CBA Kits (Fig. 3). LPS (100 ng/mL) was used as a positive control for cell activation, and non-treated cells were used as a negative control.

LPS, also called endotoxin, is a very potent inducer of inflammatory cytokines and considered to be a very common contaminant in nanoparticle formulations. Therefore, it is important to measure endotoxin levels in metallofullerenol particles in order to resolve the effect of endotoxin on the production of cytokines. The LAL test is extremely sensitive in determining the presence of free LPS and even its detection of free LPS is at the pg/mL level [24]. According to the procedure of LAL test described in the Chinese Pharmacopoeia, the endotoxin content of 100 μM Gd@$C_{82}(OH)_{22}$ aqueous solution was less than 0.125 EU/mL (0.025 ng/mL) and recorded as (−) as on the basis of the endotoxin limits in parenteral solution.

Concentrations of IL-2, IL-4, IL-5, IL-6 and IFN-γ were quite low (below 15 pg/mL) in culture supernatants of T lymphocytes and macrophages (Fig. 3A and C). Gd@$C_{82}(OH)_{22}$ nanoparticle treatments resulted in significantly higher levels of all pro-inflammatory cytokines, including Th1-related cytokines (IL-2, IFN-γ and TNF-α) and Th2 related cytokines (IL-4, IL-5 and IL-6) ($p < 0.05$). Levels of TNF-α were particularly high ($p < 0.01$) (Fig. 3B and D), in a still more concrete manner, the TNF-α content of macrophages and T cells was elevated to 125.6 ± 0.7 pg/mL and 145.0 ± 0.5 pg/mL in Gd@$C_{82}(OH)_{22}$ nanoparticle-treated groups. However, it is notable that both ELISA and CBA were unable to detect the release of cytokines in culture supernatants of B cells (data not shown). Therefore, B cells secreted very few cytokines in the presence or absence of Gd@$C_{82}(OH)_{22}$ nanoparticle stimulation.

3.3.2. Immune response of Gd@$C_{82}(OH)_{22}$

In parallel, we also tested whether pre-incubation of T lymphocytes and macrophages with Gd@$C_{82}(OH)_{22}$ nanoparticles would affect their capacity to respond further to a physiological stimulus, i.e., LPS. For this purpose, we incubated purified T lymphocytes with 100 μM Gd@$C_{82}(OH)_{22}$ nanoparticles for 24 h. LPS was then added to the wells at suboptimal concentrations (100 ng/mL) to visualize any alterations in cell response. Culture supernatants were collected 24 h later for cytokine measurement.

As shown in Fig. 3A and 3B, Gd@$C_{82}(OH)_{22}$ nanoparticles enhanced the capacity of T lymphocytes to respond to LPS-induced cytokine secretion. Levels of IL-2, IL-4, IL-5, IL-6, TNF-α and IFN-γ from co-treated T cells were significantly higher than those of LPS- or Gd@$C_{82}(OH)_{22}$ nanoparticle-treated cells ($p < 0.05$). In particular, the TNF-α content (314.8 ± 0.8 pg/mL) was almost the sum of that of LPS-treated (126.6 ± 0.7 pg/mL) and Gd@$C_{82}(OH)_{22}$ nanoparticle-treated (145.0 ± 0.5 pg/mL) groups together ($p < 0.01$). It should be noted that the TNF-α secretory capacity of both T lymphocytes and macrophages was remarkably higher than that for IL-2, IL-4, IL-5, IL-6 and IFN-γ.

However, the response of macrophages to LPS was not significantly influenced by co-culture with Gd@$C_{82}(OH)_{22}$ nanoparticles except for the secretion of TNF-α (Fig. 3C and 3D). Levels of IL-2,

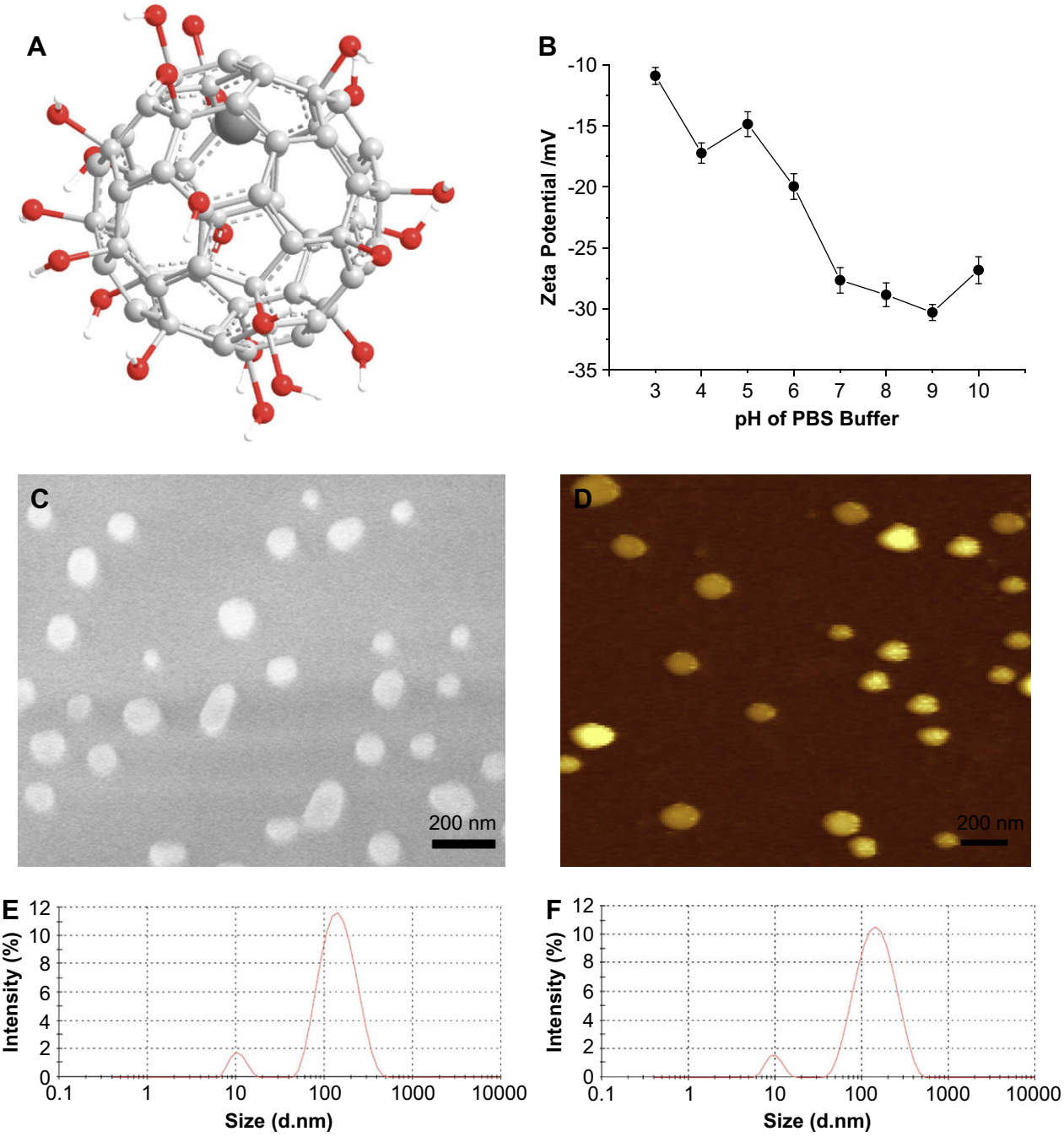

Fig. 1. Structure and characterization of Gd@$C_{82}(OH)_{22}$ nanoparticles. A is the schematic drawing of the structure of Gd@$C_{82}(OH)_{22}$ using Chem3D Ultra (Cambridge Soft). The average number of hydroxyls in the molecule is 22. Red balls represent OH groups on the fullerene surface, light gray balls represent C atoms and the large dark gray ball inside the hollow fullerene cage represents Gd. B showed the effect of lowering the pH from 7.0 to 3.0 and of increasing the pH from 7.0 to 10.0 on the zeta potentials of Gd@$C_{82}(OH)_{22}$ nanoparticles prepared in 0.01 M PBS. Both the lowering and increasing pH would induce an increase of zeta potentials of Gd@$C_{82}(OH)_{22}$ nanoparticles. These results indicated that the Gd@$C_{82}(OH)_{22}$ nanoparticles were stable in PBS of pH 7.0, 8.0, 9.0 and only became unstable under lower or higher pH conditions. Gd@$C_{82}(OH)_{22}$ tended to aggregate in aqueous solutions (pH 7.0) and formed dispersed Gd@$C_{82}(OH)_{22}$ nanoparticles with an average diameter of 100 nm as determined by SEM (C) and AFM (D). The size of the Gd@$C_{82}(OH)_{22}$ nanoparticles was stable in the physiological media in months, which was proved using dynamic light scattering (DLS). The average diameters of Gd@$C_{82}(OH)_{22}$ nanoparticles before and after being kept for a month were 154.0 ± 68.5 nm (E) and 157.5 ± 76.4 nm (F), respectively.

IL-4, IL-5, IL-6 and IFN-γ of co-treated macrophages did not change significantly compared with those for LPS-treated or Gd@$C_{82}(OH)_{22}$ nanoparticle-treated cells. TNF-α content (152.0 ± 0.5 pg/mL) of co-treated macrophages was higher than LPS-treated (35.9 ± 0.5 pg/mL) or Gd@$C_{82}(OH)_{22}$ nanoparticle-treated (125.6 ± 0.7 pg/mL) macrophages ($p < 0.01$), indeed the TNF-α content was almost the sum of that from both these treatments.

3.4. Low cytotoxicity of Gd@$C_{82}(OH)_{22}$

In this study, cell viability was assessed by trypan blue exclusion. LLC cells, B cells, T cells and macrophages were cultured in the presence of Gd@$C_{82}(OH)_{22}$ nanoparticles to assess direct stimulatory effects. We did not observe any apparent loss of living cells upon incubation of the tumor cells and three primary cell types with

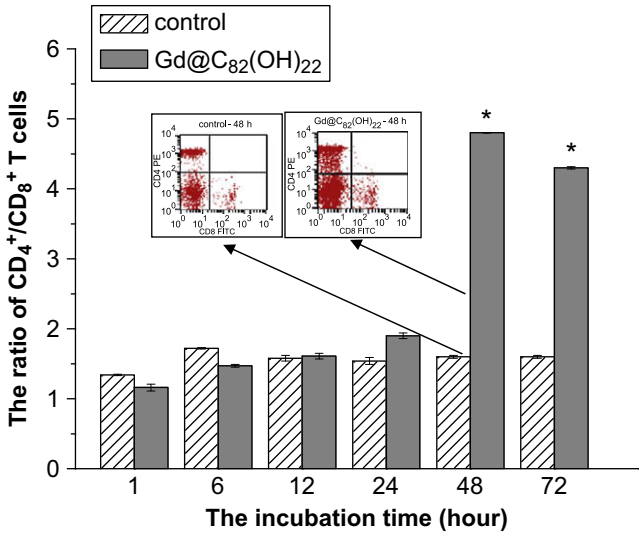

Fig. 2. The ratio of CD_4^+ to CD_8^+ T cells increased markedly after total spleen cells were incubated for 48 h and 72 h. Each bar/value represents the mean of triplicate results from three culture wells. Data are derived from one representative experiment out of three. Statistical significance (Student's *t* test) is indicated by: $^*p < 0.05$ (compared to control cells). The inner figure shows the ratio of CD_4^+ to CD_8^+ T cells analyzed by flow cytometry.

different concentrations of $Gd@C_{82}(OH)_{22}$ nanoparticles (0.1 μM, 1 μM, 10 μM and 100 μM), for 1 h, 6 h, 12 h, 24 h, 48 h and even 72 h compared with untreated cells. Cell viability was always found to be about 96–98% at the beginning and the end time points of the assays.

Another functional characteristic of tumor cells and lymphocytes is their ability to proliferate when they are activated. Compared to untreated cells, there was no apparent loss in living cells found after incubation with different concentrations of $Gd@C_{82}(OH)_{22}$ nanoparticles (0.1 μM, 1 μM, 10 μM and 100 μM), for 1 h, 6 h, 12 h, 24 h, 48 h and 72 h ($p > 0.05$) (Fig. 4).

To further confirm the effect of $Gd@C_{82}(OH)_{22}$ nanoparticles on tumor cells and primary immune cells, Beckman Coulter Cell Lab Quanta™ SC (annexin V staining combined with PI incorporation) was employed to quantify apoptotic cells. LLC cells, B cells, T cells and macrophages were incubated with $Gd@C_{82}(OH)_{22}$ nanoparticles at a concentration of 100 μM for 72 h. The apoptotic rate of LLC cells was $6.9 \pm 2.6\%$ and that of the control group was $6.5 \pm 2.4\%$, B cells was $7.1 \pm 1.2\%$ and $6.9 \pm 1.5\%$. T cells and their controls had an apoptotic rate of $8.8 \pm 0.9\%$ and $9.1 \pm 1.9\%$, respectively, while macrophages and their controls had an apoptotic rate of $10.2 \pm 1.7\%$ and $10.0 \pm 1.3\%$, respectively. No significant differences ($p > 0.05$) were observed.

Therefore, results clearly indicate that $Gd@C_{82}(OH)_{22}$ nanoparticles have low cytotoxicity and do not affect the viability and proliferation of LLC cells and primary immune cells. $Gd@C_{82}(OH)_{22}$ nanoparticles did not induce apoptosis of tumor cells and primary immune cells at or below the test dose of 100 μM and during an incubation period of at least 72 h.

3.5. Inhibition of tumor growth by $Gd@C_{82}(OH)_{22}$

In the experiment, we exactly measured the animal weights before tumor-bearing and at the end of experiment and the organ weights of liver, spleen, kidney and lung after anatomy. *In vivo* experimental data unambiguously showed that average tumor weights for all groups were markedly different 18 days after LLC cells were implanted and water-soluble $Gd@C_{82}(OH)_{22}$ nanoparticles were administered. Tumor weights of low-dose (0.1 μmol/kg/day) and high-dose (0.5 μmol/kg/day) $Gd@C_{82}(OH)_{22}$ nanoparticle-treated groups were 1.8 ± 0.5 g and 1.7 ± 0.4 g, respectively, while mean tumor weight for the untreated saline control group was 3.1 ± 0.5 g. $Gd@C_{82}(OH)_{22}$ nanoparticles inhibited tumor growth significantly ($p < 0.05$). Average inhibition rates for $Gd@C_{82}(OH)_{22}$ nanoparticles administered at 0.1 μmol/kg/day and 0.5 μmol/kg/day were 40.2% and 45.3%, respectively (Table 1).

Meanwhile, we observed that $Gd@C_{82}(OH)_{22}$ nanoparticles did not induce systemic toxicity. During the experiment, two mice in the untreated saline group died, whilst no mice in $Gd@C_{82}(OH)_{22}$ nanoparticle-treated groups died and they all were in good physiological condition. The mice body weight with and without tumor tissue were measured, and no remarkable differences have been found among the mean organ weight coefficients (%) of each of the three tumor-bearing groups (data not shown) as well as the tumor-excluded body weight thereof ($p > 0.05$). Spleen weight coefficient (%) for the untreated saline group and the $Gd@C_{82}(OH)_{22}$ nanoparticle-treated groups was greater than for the normal control. Mice body weight weeded out tumors of low-dose (0.1 μmol/kg/day) and high-dose (0.5 μmol/kg/day) $Gd@C_{82}(OH)_{22}$ nanoparticle-treated groups was 18.1 ± 0.6 g and 17.7 ± 0.9 g, respectively, while that of the untreated saline control group was 18.0 ± 0.7 g (Table 2). Although mice body weight with tumor of low-dose and high-dose nanoparticle-treated groups was lower than that of the untreated saline group, it had to been pointed that tumor weight of the two groups was less than the untreated saline group. The concentrations of Gd in the tumor tissue measured by ICP-MS were 7.0 ± 1.3 and 40.4 ± 4.1 ng/g tumor wet weight in two $Gd@C_{82}(OH)_{22}$ nanoparticle-treated groups at the dose of 0.1 and 0.5 μmol/kg/day, respectively, which corresponded to about 0.37% and 0.39% of the injected dose. It is similar to the results obtained from previous experiment [8]. That is to say, $Gd@C_{82}(OH)_{22}$ nanoparticles did not induce systemic toxicity, and the mechanism of tumor inhibition was not that $Gd@C_{82}(OH)_{22}$ directly destroyed tumor cells.

3.6. Histological findings

HE staining of tumor tissues from mice in the untreated saline group (A and B), and the 0.1 (C and D) and 0.5 (E and F) μmol/kg/day $Gd@C_{82}(OH)_{22}$ nanoparticle-treated groups is shown in Fig. 5. Numerous folliculus lymphaticus was observed in the $Gd@C_{82}(OH)_{22}$ nanoparticle-treated groups. Significant formation of envelopes composed of lymphadenoid and fibrous connective tissue surrounding the tumor tissue was observed in $Gd@C_{82}(OH)_{22}$ nanoparticle-treated groups, and is associated with lymphopoiesis. Here, lymphocyte infiltration (mainly neutrophil cells) was observed in fibroblasts with some tumor cells inside. Meanwhile, no symptom indicated acute or chronic toxicity, e.g., apoptosis, necrosis of main organs or even tumor cells. However, in the untreated saline group tumor cells proliferated heavily, arrayed regularly, and invaded the surrounding musculature (A and B) extensively. The folliculus lymphaticus and envelopes were not found. Thus, tumor-infiltrating lymphatic resistance was enhanced after treatment by $Gd@C_{82}(OH)_{22}$ nanoparticles.

3.7. Enhancement of immunity in vivo by $Gd@C_{82}(OH)_{22}$

In this study, expression of Th1 cytokines (IL-2, IFN-γ and TNF-α) and Th2 cytokines (IL-4 and IL-5) in mouse tumor tissues and serum was measured using BD Mouse Th1/Th2 Cytokine CBA Kits.

Levels of IL-2, IL-4 and IL-5 were found to be quite low in 10% tumor homogenates (Fig. 6A). In comparison to the untreated saline group, levels of Th1-related cytokines (IFN-γ and TNF-α) and Th2 related cytokines (IL-4 and IL-5) in the 0.5 μmol/kg/day

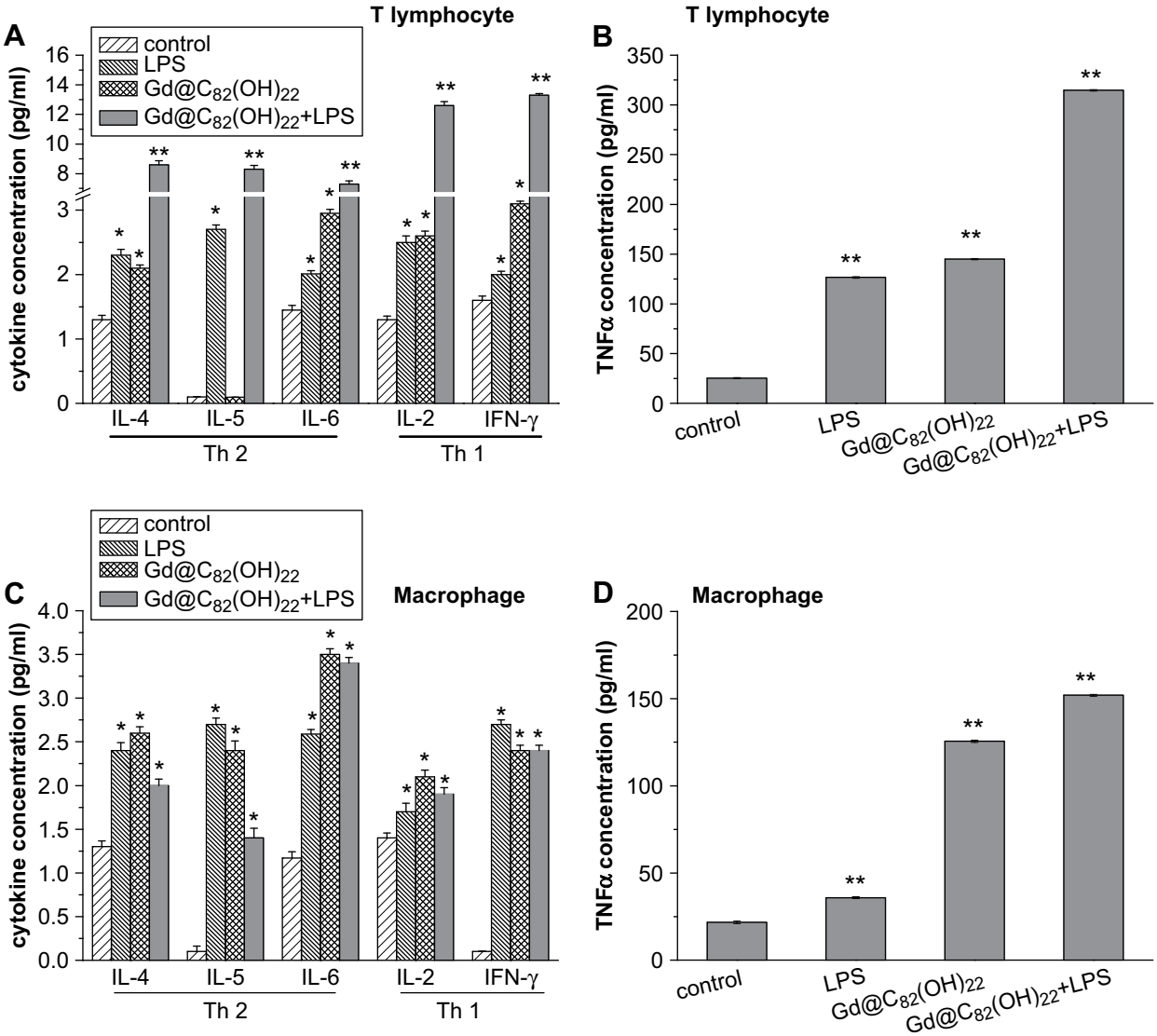

Fig. 3. $Gd@C_{82}(OH)_{22}$ nanoparticles can directly affect cytokine secretion, and incubation of T lymphocytes and macrophages with $Gd@C_{82}(OH)_{22}$ nanoparticles further affects their capacity to respond to LPS-induced cytokine secretion. LPS (0.1 μg/mL) was used as a positive control for T lymphocyte and macrophage activation. Cell culture supernatants were diluted 1:5 and analyzed by flow cytometry using a CBA inflammation kit for quantitative determination of cytokines IL-2, IL-4, IL-5, IL-6 IFN-γ and TNF-α. Each bar represents the mean of three independent samples. (A) IL-2, IL-4, IL-5, IL-6 and IFN-γ levels of T cell culture supernatants; (B) TNF-α levels of T cell culture supernatants; (C) IL-2, IL-4, IL-5, IL-6 and IFN-γ levels of macrophage culture supernatants; (D) TNF-α levels of macrophage culture supernatants. Statistical significance (Student's *t* test) is indicated by: $^{*}p < 0.05$, $^{**}p < 0.01$ (compared to untreated cells).

$Gd@C_{82}(OH)_{22}$ nanoparticle-treated group increased significantly ($p < 0.01$). However, no marked alteration of cytokines was detected in the low-dose (0.1 μmol/kg/day) $Gd@C_{82}(OH)_{22}$ nanoparticle-treated group ($p > 0.05$).

Cytokine levels in mouse serum were different from those in the 10% tumor homogenate (Fig. 6B). Levels of both Th1 cytokines and Th2 cytokines in all the tumor-bearing groups increased significantly compared to the normal control group. However, compared to the untreated saline group, levels of Th1 cytokines (IL-2, IFN-γ and TNF-α) increased significantly, while Th2 cytokines (IL-4 and IL-5) decreased in both the 0.1 and 0.5 μmol/kg/day $Gd@C_{82}(OH)_{22}$ nanoparticle-treated groups ($p < 0.05$ and $p < 0.01$, respectively).

Fig. 6 shows clearly that TNF-α content was higher than that of any other cytokines (IL-2, IL-4, IL-5 and IFN-γ) in both tumor tissues and serum. In the group treated with the higher dose of nanoparticles, the TNF-α content of the tumor homogenate was 954.3 ± 17.0 pg/mg protein compared with 544.1 ± 34.6 pg/mg protein in the saline group, and that of the serum was 407.7 ± 72.4 pg/mg protein compared with 181.5 ± 37.1 pg/mg protein in the saline group. $Gd@C_{82}(OH)_{22}$ nanoparticle-treated groups consistently had about double the TNF-α content of the saline control in both tumor homogenates and serum. These results indicate that the capability of $Gd@C_{82}(OH)_{22}$ nanoparticles to inhibit tumor growth was accomplished by inducing TNF-α mediated cellular immunity.

4. Discussion

The immune system is one of the most important means by which animals protect themselves from external threats and plays a critical role in surveillance and prevention of malignancy [25]. It is only when malignant cells develop mechanisms to escape the immune system that they become clinically significant tumors. The present *in vivo* and *in vitro* studies indicate that $Gd@C_{82}(OH)_{22}$ nanoparticles can inhibit tumor growth efficiently and appear to neither affect cell

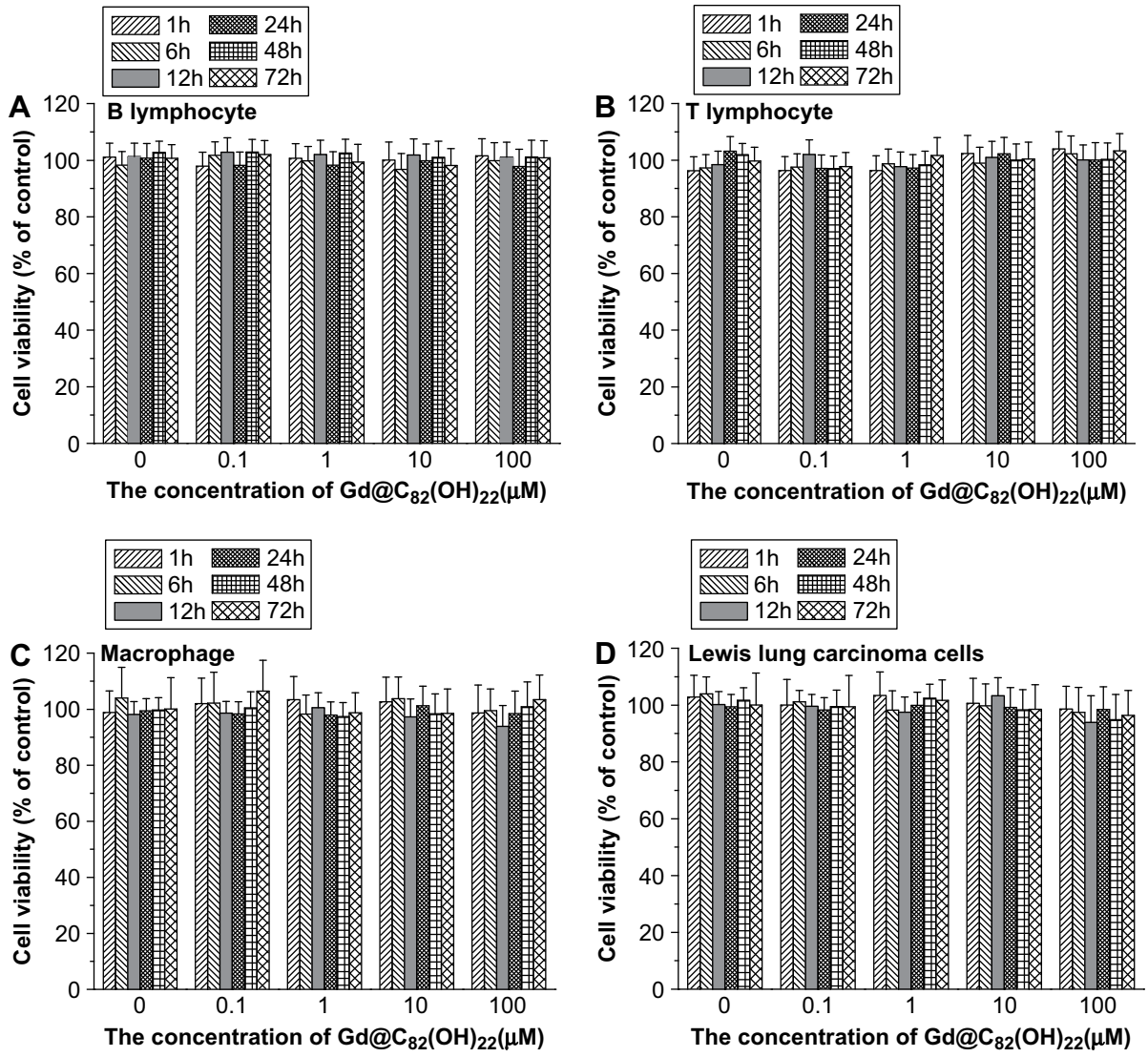

Fig. 4. $Gd@C_{82}(OH)_{22}$ nanoparticles have no effect on immune cells and tumor cells (LLC cells) viability. A, B cells; B, T cells; C, macrophages; D, LLC cells. Separated cells were measured immediately using cell count kit-8. 100% is that the concentration of $Gd@C_{82}(OH)_{22}$ nanoparticles in the incubation solution was 0 μM and time of incubation was 0 h. Each bar/value represents the mean of triplicate results from three culture wells. Data are derived from one representative experiment out of three.

viability nor proliferation of lymphocytes and macrophages. Attention in this study has been focused on the stimulation of immune cells by $Gd@C_{82}(OH)_{22}$ nanoparticles to release cytokines.

Cytokine is a kind of small proteins synthesized and secreted by immune cells (such as mononuclear phagocyte, T cell, B cells, NK cells, etc.) and some non-immune cells (such as vascular endothelial cells, epidermal cells, fibroblasts, etc.). As a kind of molecule for cell signal transduction, cytokines mainly regulate immune response, participate in immune cell differentiation and development, mediate inflammatory response and stimulate the hematopoietic function and tissue repair [26].

Table 1
Anti-tumor activity of $Gd@C_{82}(OH)_{22}$ nanoparticles in mice bearing LLC.

Group and dosage	Tumor weight (g) (mean ± SD)	*t*-test	Inhibition rate (%)
Normal control ($n = 10$)	–	–	–
Untreated saline group ($n = 10$)	3.1 ± 0.5	–	–
$Gd@C_{82}(OH)_{22}$ group (0.1 μmol/kg/day, $n = 10$)	1.8 ± 0.5	$p < 0.05$	40.2
$Gd@C_{82}(OH)_{22}$ group (0.5 μmol/kg/day, $n = 10$)	1.7 ± 0.4	$p < 0.05$	45.3

It is a complicated process that cytokines are secreted and transported to the tumor tissues. It may mainly include the following ways: (1) At the early stage of cancer progression or tumor cell inoculation, there are a small number of leukocytes, macrophages, fibroblasts and lymphocyte, which can release all kinds of cytokines around the tumor cells. However, the infiltration response will disappear soon because the tumor extracellular matrix and tumor cells can produce prostaglandin E2 (PGE2), transforming growth factor β (TGF-β), interleukin-10 (IL-10) and other factors to suppress the function of the above infiltrating inflammatory cells. An effective anti-tumor mechanism is unable to set up, which results in restriction of tumor growth [27]. (2) Once an immune response is stimulated, large quantities of cytokines secreted by immune cells such as lymphocytes, granulocyte cells, macrophages and other cells such as fibroblasts, epithelial cells, are released into the blood circulation and then transported to tumor tissue. These are the main sources of the cytokines in the tumor

Table 2
$Gd@C_{82}(OH)_{22}$ nanoparticles have low influence on the body weight of tumor-bearing mice.

Group and dosage	Body weight before tumor-bearing (g)	Body weight before sacrifice (g)	Tumor weight (g)	Body weight without tumor (g)	Content of Gd (ng/tumor wet weight)
Normal control ($n = 10$)	18.9 ± 0.7	20.5 ± 0.7	–	–	–
Untreated saline group ($n = 10$)	19.2 ± 0.8	21.1 ± 1.0	3.1 ± 0.5	17.9 ± 0.7	1.1 ± 0.3
$Gd@C_{82}(OH)_{22}$ group (0.1 μmol/kg/day, $n = 10$)	18.9 ± 1.2	$20.3 \pm 1.2^{*}$	$1.8 \pm 0.5^{*}$	18.1 ± 0.6	7.0 ± 1.3
$Gd@C_{82}(OH)_{22}$ group (0.5 μmol/kg/day, $n = 10$)	18.8 ± 0.7	$20.0 \pm 1.0^{**}$	$1.7 \pm 0.4^{*}$	17.7 ± 0.9	40.4 ± 4.0

Statistical significance (student's t test) is indicated by: $^{*}p < 0.05$, $^{**}p < 0.01$.

tissue [28]. (3) During the development of tumor, tumor-infiltrating cells (TIL), consisting of activated T cells, NK cells, non-T and non-B cells, can release several cytokines, such as TNF-α and IFN-γ [29,30].

Herein, the direct impact of $Gd@C_{82}(OH)_{22}$ nanoparticles on primary cells belonging to the immune system is reported for the first time. $Gd@C_{82}(OH)_{22}$ nanoparticles can activate cell functions (as shown by the stimulation of pro-inflammatory cytokine secretion) and modulate their subsequent capacity to respond to a physiological stimulus. Different types of mouse immune cells were separated and incubated with $Gd@C_{82}(OH)_{22}$ nanoparticles

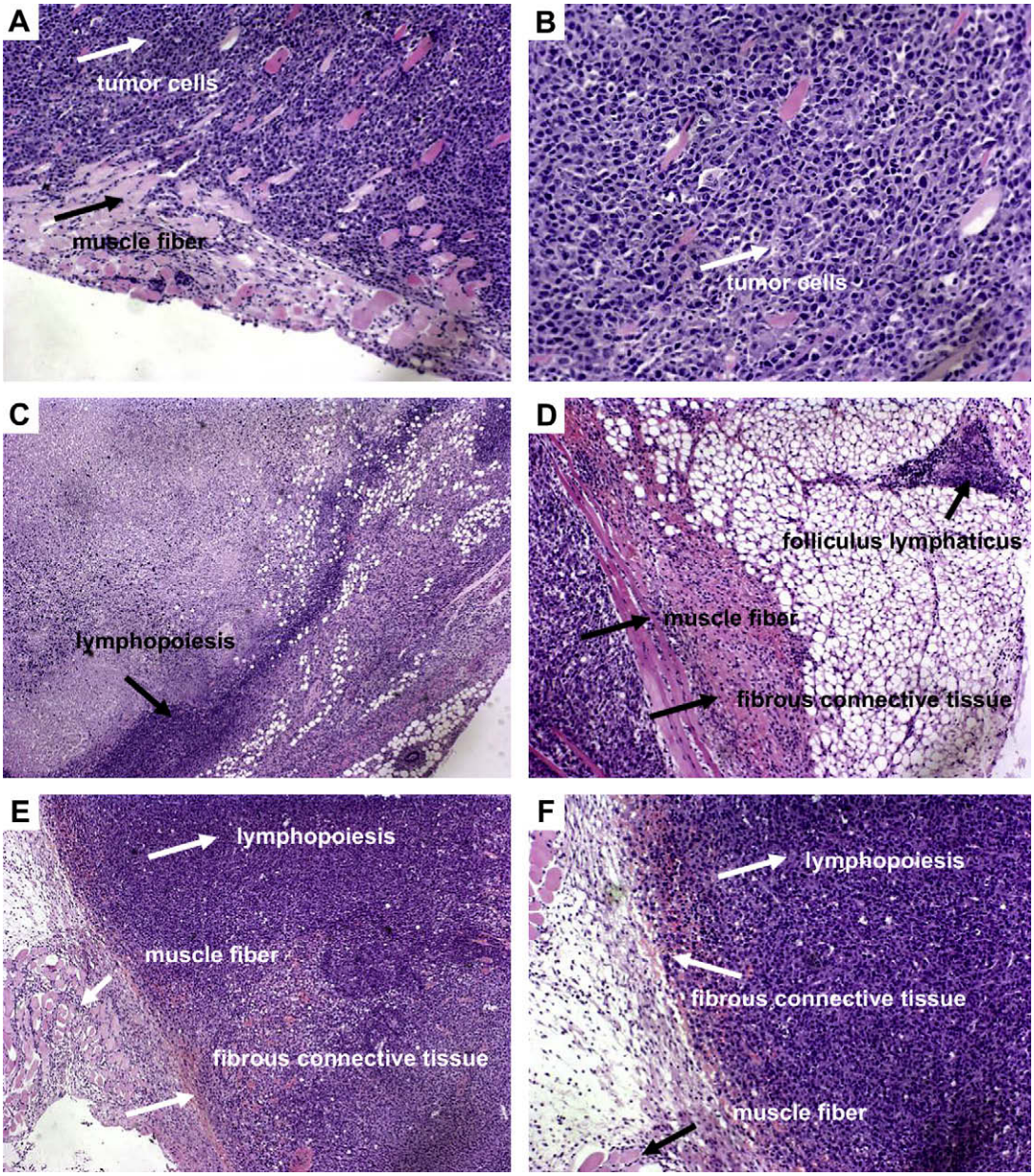

Fig. 5. HE staining of tumor tissues from mice in the untreated saline group (A and B), 0.1 μmol/kg/day $Gd@C_{82}(OH)_{22}$ nanoparticle-treated group (C and D) and 0.5 μmol/kg/day $Gd@C_{82}(OH)_{22}$ nanoparticle-treated group (E and F). Large numbers of folliculus lymphaticus were observed in the $Gd@C_{82}(OH)_{22}$ nanoparticle-treated groups (C, D, E, F arrows). Significant formation of envelopes surrounding tumor tissues composed of lymphadenoid and fibrous connective tissue, indicative of lymphopoiesis, was observed in the $Gd@C_{82}(OH)_{22}$ nanoparticle-treated groups (D, E, F arrows). (Original magnification: C and E, ×50; A, D and F, ×100; B, ×200).

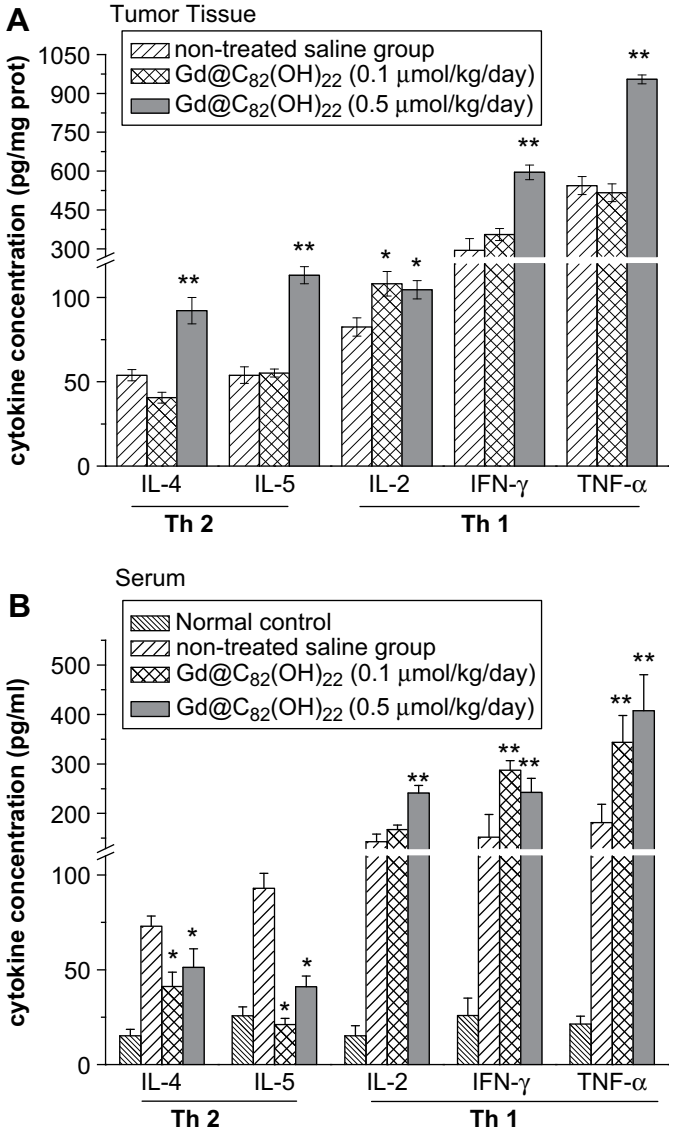

Fig. 6. The immune system can be activated by water-soluble $Gd@C_{82}(OH)_{22}$ nanoparticles *in vivo*. Cytokines, including IL-2, IL-4, IL-5, TNF-α and IFN-γ were measured quantitatively, in mouse tumor tissues and serum using the mouse Th1/Th2 cytokine CBA kit. (A) In comparison to the untreated saline group, IFN-γ and TNF-α expression levels in mouse tumor tissues increased markedly in the group treated with 0.5 μmol/kg/day $Gd@C_{82}(OH)_{22}$ nanoparticles. (B) IFN-γ, TNF-α and IL-2 expression levels in mouse serum increased in the $Gd@C_{82}(OH)_{22}$ nanoparticle-treated group while IL-4, IL-5 expression levels decreased. Statistical significance (Student's *t* test) is indicated by: $^{*}p < 0.05$, $^{**}p < 0.01$.

and the effects of this fullerene derivative on cytokine secretion were investigated using flow cell cytometry, ELISA and Th1/Th2 Cytokine CBA kits. We found that $Gd@C_{82}(OH)_{22}$ nanoparticles had little effect on the activity of immune cells at very low concentrations. However, higher concentrations (such as 100 μM) markedly stimulated immune cells to release cytokines, especially TNF-α which plays a key role in the cellular immune process, in response to external signals [31].

Immune regulation relies mainly on helper T cells (CD_4^+ T) and cytotoxic T cells (CD_8^+ T), and dynamic changes in the CD_4^+/CD_8^+ ratio are regarded as an important factor in determining immunity states and levels. CD_4^+ T cells are thought to play an important role in anti-tumor immunology by regulating the differentiation and development of CD_8^+ T cells [32,33]. Optimal anti-tumor immune responses are therefore considered to require the concomitant activation of both CD_8^+ and CD_4^+ T cells and the selective activation of CD_4^+ T cells with helper but not regulatory functions [34]. Pathological studies have shown that the ratio of CD_4^+ T cells to CD_8^+ T cells in peripheral blood in tissues obtained from cancer patients decreases as the cancer becomes worse. In contrast, in the present study we observed the opposite effect as the ratio of CD_4^+ T cells to CD_8^+ T cells increased markedly after treatment, and has concluded that $Gd@C_{82}(OH)_{22}$ nanoparticles are capable of improving the immune functions of organisms, thus inhibiting tumor growth. So, subsequent studies focused on the interaction of $Gd@C_{82}(OH)_{22}$ nanoparticles and primary immune cells, including B cells, T cells and macrophages.

CD_4^+ T cells are found in two distinct cell types, Th1 and Th2, distinguished by the cytokines they produce and respond to and the immune responses they are involved in. Th1 cells mainly produce IFN-γ, IL-2 and IL-12, while Th2 lymphocytes predominantly release IL-4, IL-5, IL-13, IL-10 and IL-6. However, TNF-α can be secreted by both Th1 and Th2 cells [35,36]. The balance between Th1 and Th2 cells is associated with infectious diseases, allergic diseases, and autoimmune diseases and the progenesis, development and prognosis of cancers. It has been demonstrated that water-soluble chitosan (WSC) has specific immunomodulatory effects on macrophages including polarizing the cytokine balance towards Th1 cytokines, decreasing the production of the inflammatory cytokines IL-6 and TNF-α, down-regulating CD44 and TLR4 receptor expression, and inhibiting T cell proliferation [37]. Here, our interest was to determine the immunomodulatory effects of $Gd@C_{82}(OH)_{22}$ nanoparticles on T cells and macrophages.

$Gd@C_{82}(OH)_{22}$ nanoparticles induced inflammatory cytokine secretion *in vitro*, and up-regulated the immune response. We previously hypothesized that $Gd@C_{82}(OH)_{22}$ nanoparticles may improve the immune system of tumor-bearing mice [8]. In our *in vivo* experiments, when LLC cells were injected into the upper right hind leg of mice, results were similar to those of our previous reports. Numerous folliculus lymphaticus were observed in the $Gd@C_{82}(OH)_{22}$ nanoparticle-treated group. Significant numbers of envelopes composed of lymphadenoid and fibrous connective tissue surrounded tumor tissues in the $Gd@C_{82}(OH)_{22}$ nanoparticle-treated group, indicating the occurrence of lymphopoiesis. However, tumor cells proliferated heavily, arrayed regularly, and invaded the surrounding musculature extensively in the untreated saline group. The results of these two *in vivo* experiments show that $Gd@C_{82}(OH)_{22}$ nanoparticles have a similar role in different tumor models. It is presumed that $Gd@C_{82}(OH)_{22}$ nanoparticles encounter a complex environment immediately after entering the blood stream, and may be taken up by immune cells both in the blood stream (monocytes, platelets, leukocytes and dendritic cells (DC)), and in tissues by resident phagocytes (e.g. Kupffer cells in liver, DC in lymph nodes, macrophages and B/T cells in spleen) via specific and nonspecific phagocytic pathways.

In this study, the mouse immune system, stimulated by $Gd@C_{82}(OH)_{22}$ nanoparticles, was found to release significantly higher levels of Th1 cytokines (TNF-α, IFN-γ and IL-2), but only small quantities of Th2 cytokines (IL-4, IL-5, and IL-6). An interesting phenomenon was uncovered in our CBA assay conducted to measure the IL-2, IL-4, IL-5, TNF-α and IFN-γ levels in mice serum; $Gd@C_{82}(OH)_{22}$ nanoparticle-treated groups showed increased levels of IFN-γ, TNF-α and IL-2 levels and decreased levels of IL-4, and IL-5. It is clear that tumors can cause Th1 cell responses to drift to Th2 cell responses. In our experiments $Gd@C_{82}(OH)_{22}$ nanoparticles were able to promote T cells to differentiate into Th1 cells, moving the Th1/Th2 balance to the Th1 side in mice with lung cancer.

At the same time, we found that the IL-2, IL-4, IL-5, TNF-α and IFN-γ levels of $Gd@C_{82}(OH)_{22}$ nanoparticle-treated groups were all

higher than the untreated saline group in mouse tumor tissue. TIL (tumor infiltration lymphocyte) cells may play an important role to regulate the level of cytokines. Both CD_4^+ and CD_8^+ TIL cells were highly activated to prevent tumor progression in tumor tissue. TIL populations have the capacity to secrete cytokines or kill tumor cells by releasing immunoregulatory cytokines such as IL-2, IL-4, IL-10, GM-CSF, TNF-α, and IFN-γ [38]. Especially, Terheyden found that more CD_4^+ Th2 cells would be harvested after TIL was stimulated by DC cells and tumor lysate in vitro [39]. In our experiment, we hypothesized that TIL was stimulated to differentiate more CD_4^+ Th2 cells than Th1 cells in tumor tissue, resulted in Th2 cytokines levels increasing. Meanwhile, the function of $Gd@C_{82}(OH)_{22}$ nanoparticles promoting T cells to differentiate into Th1 cells and moving the Th1/Th2 balance to the Th1 side still existed and performed an important function. However, the mechanism of $Gd@C_{82}(OH)_{22}$ nanoparticle-mediated immunostimulation and the identity of primary immune cells activated that lead to different immunological responses are not clear. Factors such as the administration route and particle size, may account for the Th1 vs. Th2 response to $Gd@C_{82}(OH)_{22}$ nanoparticles, and will be investigated in further studies.

One notable finding is that the level of TNF-α in $Gd@C_{82}(OH)_{22}$ nanoparticle-treated groups appeared to increase markedly both *in vivo* and *in vitro*. TNF-α was originally identified for its capacity to induce hemorrhagic necrosis of solid tumors, and to inhibit the interaction of integrin with other drugs at the molecular level to trigger apoptosis and dissociation of tumor vascular endothelial cells [40], and is now recognized as a pleiotropic cytokine that is indispensable in multiple biological processes. As reported previously [41], TNF-α can induce the apoptosis and death of tumor cells as well as viruses by binding to the target tumor necrosis factor receptor (TNFR) on the cell membrane. Under suboptimal immunostimulatory conditions, TNF-α −/− animals display multiple T cell intrinsic and T cell extrinsic defects, which differentially rely on TNFR1 and TNFR2 mediated signals. These defects ultimately result in impaired anti-tumor immunity due to defective activation, proliferation, and recruitment of tumor-specific CD_8^+ T cells. In our study, some notable examples of tumor cell apoptosis were observed using transmission electron microscopy, such as chromatin enrichment, endoplasmic reticulum distension and microvillus disappearance (data not shown). The downstream NF-κB signaling pathway may play a role in this process [42,43]. TNF-α can up-regulate the expression of CCL2 and adhesion molecules of human proximal tubular epithelial cells through MAPK signaling pathways [44]. These inflammatory molecules and underlying intracellular signaling molecules are potentially useful therapeutic targets for investigating the anti-tumor mechanism of $Gd@C_{82}(OH)_{22}$ nanoparticles.

Meanwhile, taking all our results into account, we suggest a mechanism involving several possible immune-associated pathways by which water-soluble $Gd@C_{82}(OH)_{22}$ nanoparticles inhibit the growth of tumors (Fig. 7). Macrophages may play an indispensable role for triggering, instructing and modulating the adaptive immune response in these ways. The $Gd@C_{82}(OH)_{22}$ nanoparticles injected in the abdominal cavity are mostly engulfed by macrophages and other phagocytes through phagocytosis, whilst a few enter the blood directly through the peritoneum or mesentery. Then the $Gd@C_{82}(OH)_{22}$ nanoparticles stimulate macrophages and T cells to release several kinds of cytokines, such as, IL-2, IL-4, IL-5, TNF-α and IFN-γ. At the same time, macrophages collaborate with T cells both through cell-to-cell interactions and by which they can be activated. Large quantities of cytokines released into the blood, and the central (thymus gland) and peripheral lymphatic systems (of which the spleen is the largest and most important) are activated. Th0 cells differentiate into Th1 and Th2 cells. $Gd@C_{82}(OH)_{22}$ nanoparticles may stimulate Th0 cells to differentiate proportionately more Th1 cells that release more IFN-γ, TNF-α and IL-2. Cytokines are focused to tumor tissue by the blood, TNF-α then triggers a series of signal pathways to promote tumor cell apoptosis. The activated TIL in tumor tissues can kill tumor cells directly by releasing IL-2.

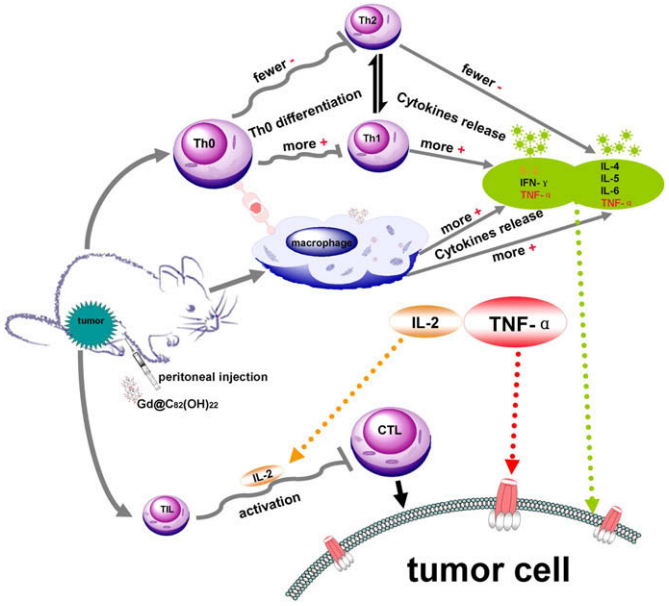

Fig. 7. Possible immune-associated pathways by which $Gd@C_{82}(OH)_{22}$ nanoparticles inhibit the growth of tumors. The $Gd@C_{82}(OH)_{22}$ nanoparticles injected in the abdominal cavity are mostly engulfed by macrophages and other phagocytes through phagocytosis, whilst a few enter the blood directly through the peritoneum or mesentery. Then the $Gd@C_{82}(OH)_{22}$ nanoparticles stimulate macrophages and T cells to release several kinds of cytokines, such as, IL-2, IL-4, IL-5, TNF-α and IFN-γ. At the same time, macrophages collaborate with T cells both through cell-to-cell interactions and by which they can be activated. Large quantities of cytokines released into the blood, and the central (thymus gland) and peripheral lymphatic systems (of which the spleen is the largest and most important) are activated. Th0 cells differentiate into Th1 and Th2 cells. $Gd@C_{82}(OH)_{22}$ nanoparticles may stimulate Th0 cells to differentiate proportionately more Th1 cells that release more IFN-γ, TNF-α and IL-2. Cytokines are focused to tumor tissue by the blood, TNF-α then triggers a series of signal pathways to promote tumor cell apoptosis. The activated TIL in tumor tissues can kill tumor cells directly by releasing IL-2.

The use of $Gd@C_{82}(OH)_{22}$ nanoparticles as a potential anti-tumor medicine may have bright prospects. In addition to their low-toxicity and high-efficiency in inhibiting tumor growth, we have demonstrated the ability of $Gd@C_{82}(OH)_{22}$ nanoparticles to up-regulate the immune system in contrast to the immune-suppressing effects of conventional radiotherapy and chemotherapy. While the mechanism of action still requires further confirmation, our results warrant further investigation of the effects of $Gd@C_{82}(OH)_{22}$ nanoparticles on the immune system, especially on tumor cell apoptosis and death mediated by TNF-α. At the same time, the effect of $Gd@C_{82}(OH)_{22}$ nanoparticles on enhancing the efficacy of other anticancer drugs and counteracting their side effects deserves further study.

5. Conclusion

Our results show that in addition to its Th1 adjuvanticity, $Gd@C_{82}(OH)_{22}$ nanoparticles are a strong immunomodulator of the activation of T cells and macrophages. $Gd@C_{82}(OH)_{22}$ nanoparticles play important roles in the anti-tumor process by activating the immune system including polarizing the cytokine balance towards Th1 cytokines, decreasing the production of Th2 cytokines, and increasing the production of Th1 cytokines. $Gd@C_{82}(OH)_{22}$

nanoparticles could effectively help the immune system to scavenge tumor cells, and thus depress the viability of tumor tissues by activating TNF-α mediated cellular immunity. Gd@$C_{82}(OH)_{22}$ nanoparticles may provide a good therapeutic modality for solid tumors.

Acknowledgment

This work is financially supported by the Ministry of Science and Technology of the People's Republic of China (2006CB705603, 2008ZX10104 and 2009AA03J335), the National Natural Science Foundation of China (20751001), the National Science Foundation for Distinguished Young Scholars (10525524), the Knowledge Innovation Program of the Chinese Academy of Sciences (KJCX2-YW-M02), and the Chinese Academy of Sciences K.C. Wong Post-doctoral Fellowships.

Appendix

Figures with essential colour discrimination. Certain figures in this article, in particular parts of Figures 1, 2, 5 and 7, are difficult to interpret in black and white. The full colour images can be found in the on-line version, at doi:10.1016/j.biomaterials.2009.04.001.

References

[1] Jordan JT, Sun W, Hussain SF, DeAngulo G, Prabhu SS, Heimberger AB. Preferential migration of regulatory T cells mediated by glioma-secreted chemokines can be blocked with chemotherapy. Cancer Immunol Immunother 2008;57:123–31.
[2] Dobrovolskaia MA, Aggarwal P, Hall JB, McNeil SE. Preclinical studies to understand nanoparticle interaction with the immune system and its potential effects on nanoparticle biodistribution. Mol Pharm 2008;5:487–95.
[3] Kroto HW, Heath JR, O'Brien SC, Curl RF, Smalley RE. C(60): buckminsterfullerene. Nature 1985;318:162–3.
[4] Bosi S, Da Ros T, Spalluto G, Prato M. Fullerene derivatives: An attractive tool for biological applications. Eur J Med Chem 2003;38:913–23.
[5] Tabata Y, Ikada Y. Biological functions of fullerene. Pure Appl Chem 1999;71:2047–53.
[6] Tabata Y, Murakami Y, Ikada Y. Photodynamic effect of polyethylene glycol-modified fullerene on tumor. Jpn J Cancer Res 1997;88:1108–16.
[7] Anderson SA, Lee KK, Frank JA. Gadolinium-fullerenol as a paramagnetic contrast agent for cellular imaging. Invest Radiol 2006;41:332–8.
[8] Chen C, Xing G, Wang J, Zhao Y, Li B, Tang J, et al. Multihydroxylated $[Gd@C82(OH)_{22}]_n$ nanoparticles: antineoplastic activity of high efficiency and low toxicity. Nano Lett 2005;5:2050–7.
[9] Kiselev OI, Kozeletskaya KN, Melenevskaya EY, Vinogradova LV, Kever EE, Klenin SI, et al. Antiviral activity of fullerene C60 with the poly-(*N*-vinylpyrrolidone) complex. Mol Cryst Liq Cryst Sci Technol C Mol Mater 1998;11:121–4.
[10] Cui Z, Mumper RJ. Coating of cationized protein on engineered nanoparticles results in enhanced immune responses. Int J Pharm 2002;238:229–39.
[11] Cuna M, Alonso-Sandel M, Remunan-Lopez C, Pivel JP, Alonso-Lebrero JL, Alonso MJ. Development of phosphorylated glucomannan-coated chitosan nanoparticles as nanocarriers for protein delivery. J Nanosci Nanotechnol 2006;6:2887–95.
[12] Tang J, Xing G, Yuan H, Cao W, Jing L, Gao X, et al. Tuning electronic properties of metallic atom in bondage to a nanospace. J Phys Chem B 2005;109:8779–85.
[13] Yin J, Lao F, Meng J, Fu P, Zhao Y, Xing G, et al. Inhibition of Tumor growth by polyhydroxylated endohedral metallofullerenol nanoparticles optimized as reactive oxygen species. Mol Pharmacol 2008;74:1132–40.
[14] Yin J, Lao F, Fu P, Wamer W, Zhao Y, Wang P, et al. The scavenging of reactive oxygen species and the potential for cell protection by functionalized fullerene materials. Biomaterials 2009;30:611–21.
[15] Tang J, Xing G, Zhao Y, Jing L, Gao X, Cheng Y, et al. Periodical variation of electronic properties in polyhydroxylated metallofullerene materials. Adv Mater 2006;18:1458–62.
[16] Tang J, Xing G, Zhao Y, Jing L, Yuan H, Zhao F, et al. Switchable semiconductive property of the polyhydroxylated metallofullerene. J Phys Chem B 2007;111:11929–34.
[17] State Pharmacopoeia Committee. Chinese pharmacopoeia; 2005. Second Part: 85.
[18] Ten H, Timo LM, Van VW, Bakker W, Irma AJM. Isolation and characterization of murine Kupffer cells and splenic macrophages. J Immunol Methods 1996;193:81–91.
[19] Martins EJ, Ferreira AC, Skorupa AL, Afeche SC, Cipolla-Neto J, Costa Rosa LF. Tryptophan consumption and indoleamines production by peritoneal cavity macrophages. J Leukoc Biol 2004;75:1116–21.
[20] Maeda N, Kokai Y, Ohtani S, Sahara H, Kumamoto-Yonezawa Y, Kuriyama I, et al. Anti-tumor effect of orally administered spinach glycolipid fraction on implanted cancer cells, colon-26, in mice. Lipids 2008;43:741–8.
[21] Wang J, Chen C, Li B, Yu H, Zhao Y, Sun J, et al. Antioxidative function and biodistribution of $[Gd@C82(OH)_{22}]_n$ nanoparticles in tumor-bearing mice. Biochem Pharmacol 2006;71:872–81.
[22] Kitano T, Ateshian GA, Mow VC, Kadoya Y, Yamano Y. Constituents and pH changes in protein rich hyaluronan solution affect the biotribological properties of artificial articular joints. J Biomech 2001;34:1031–7.
[23] Kitano T, Ohashi H, Kadoya Y, Kobayashi A, Yutani Y, Yamano Y. Measurements of zeta potentials of particulate biomaterials in protein-rich hyaluronan solution with changes in pH and protein constituents. J Biomed Mater Res 1998;42:453–7.
[24] Ried C, Wahl C, Miethke T, Wellnhofer G, Landgraf C, Schneider MJ, et al. High affinity endotoxin binding and neutralizing peptides based on the crystal structure of recombinant Limulus anti-lipopolysaccharide factor. J Biol Chem 1996;27:28120–7.
[25] Melvold RW, Sticca RP. Basic and tumor immunology: a review. Surg Oncol Clin N Am 2007;16:711–35.
[26] Yu J, Ren X, Cao S, Li H, Hao X. Beneficial effects of fetal-maternal microchimerism on the activated haplo-identical peripheral blood stem cell treatment for cancer. Cytotherapy 2008;10:331–9.
[27] Chang HL, Gillett N, Figari I, Lopez AR, Palladino MA, Derynck R. Increased transforming growth factor beta expression inhibits cell proliferation in vitro, yet increases tumorigenicity and tumor growth of Meth A sarcoma cells. Cancer Res 1993;53:4391–8.
[28] Knutson KL, Disis ML. Tumor antigen-specific T helper cells in cancer immunity and immunotherapy. Cancer Immunol Immunother 2005;54:721–8.
[29] Joyce BR, James CH, Richard WD, Mark JD. Type 1 and type 2 tumor infiltrating effector cell subpopulations in progressive breast cancer. Clin Immunol 2004;111:69–81.
[30] Csiszar A, Szentes T, Haraszti B, Pocsik E. Cytokine profile of human colorectal carcinoma infiltrating leukocytes (TIL) and tumor cells. Immunol Lett 2000;73:254–5.
[31] Carswell EA, Old LJ, Kassel RL, Green S, Fiore N, Williamson B. An endotoxin-induced serum factor that causes necrosis of tumors. Proc Natl Acad Sci U S A 1975;72:3666–70.
[32] Wang RF, Peng G, Wang HY. Regulatory T cells and toll-like receptors in tumor immunity. Semin Immunol 2006;18:136–42.
[33] Sakaguchi S, Setoguchi R, Yagi H, Nomura T. Naturally arising Foxp3-expressing CD25 + CD4+ regulatory T cells in self-tolerance and autoimmune disease. Curr Top Microbiol Immunol 2006;305:51–66.
[34] Leen AM, Rooney CM, Foster AE. Improving T cell therapy for cancer. Annu Rev Immunol 2007;25:243–65.
[35] Katsikis PD, Wunderlich ES, Smith CA, Herzenberg LA. Fas antigen stimulation induces marked apoptosis of T lymphocytes in human immunodeficiency virus-infected individuals. J Exp Med 1995;181:2029–36.
[36] Annunziato F, Galli G, Cosmi L, Romagnani P, Manetti R, Maggi E, et al. Molecules associated with human Thl or Th2 cells. Eur Cytokine Netw 1998;9:12–6.
[37] Chen CL, Wang YM, Liu CF, Wang JY. The effect of water-soluble chitosan on macrophage activation and the attenuation of mite allergen-induced airway inflammation. Biomaterials 2008;29:2173–82.
[38] Van den Hove LE, Van Gool SW, Van Poppel H, Baert L, Coorevits L, Van Damme B, et al. Phenotype, cytokine production and cytolytic capacity of fresh (uncultured) tumour-infiltrating T lymphocytes in human renal cell carcinoma. Clin Exp Immunol 1997;109:501–9.
[39] Terheyden P, Straten P, Bröcker EB, Kämpgen E, Becker JC. CD40-ligated dendritic cells effectively expand melanoma-specific CD8+ CTLs and CD4+ IFN-gamma-producing T cells from tumor-infiltrating lymphocytes. J Immunol 2000;164:6633–9.
[40] Lokshin A, Raskovalova T, Huang X. Adenosine-mediated inhibition of the cytotoxic activity and cytokine production by activated natural killer cells. Cancer Res 2006;66:7758–65.
[41] Thomas C, Marc P, Håkan H, Laurent S, Nobuyuki O, Alisha RE, et al. TNF-α is critical for antitumor but not antiviral T cell immunity in mice. J Clin Investig 2007;117:3833–45.
[42] Hur GM, Lewis J, Yang Q, Lin Y, Nakano H, Nedospasov S. The death domain kinase RIP has an essential role in DNA damage-induced NF-kappa B activation. Genes Dev 2003;17:873–82.
[43] Nicolas A, Cathelin D, Larmonier N, Fraszczak J, Puig PE, Bouchot A, et al. Dendritic cells trigger tumor cell death by a nitric oxide-dependent mechanism. J Immunol 2007;179:812–8.
[44] Ho AW, Wong CK, Lam CW. Tumor necrosis factor-a up-regulates the expression of CCL2 and adhesion molecules of human proximal tubular epithelial cells through MAPK signaling pathways. Immunobiology 2008;213:533–44.